

RESEARCH ARTICLE

Third generation fluoroquinolones antibacterial drug based mixed-ligand Cu(II) complexes: structure, antibacterial activity, superoxide dismutase activity and DNA–interaction approach

Mohan N. Patel, Pradhuman A. Parmar, and Deepen S. Gandhi

Department of Chemistry, Sardar Patel University, Vallabh Vidyanagar, Gujarat, India

Abstract

The copper(II) complexes of the type $[\text{Cu}(\text{SPF})(\text{A}^n)\text{Cl}]$ / $[\text{Cu}(\text{PFL})(\text{A}^n)\text{Cl}]$ (where SPF is sparfloxacin, PFL is pefloxacin and A^n is 2,2'-dipyridylamine/pyridine-2-carboxaldehyde/thiophene-2-carboxaldehyde) were synthesised and were found to have a pyramidal geometry with a square base. The superoxide dismutase (SOD) like activity of the complexes were measured using an NBT/NADH/PMS system, these were expressed in terms of the concentration of complex which terminates the formation of formazan by 50% (IC_{50} value) and found to range from 0.781 to 1.354 μM . The interactions of the complexes with DNA were studied by absorption titration, viscosity measurement and gel electrophoresis under physiological conditions. The antimicrobial efficiency of the complexes were tested on five different microorganisms and showed good biological activity.

Keywords: Square pyramidal Cu(II) complexes, spectrophotometric titration, IC_{50} , DNA binding and cleavage

Introduction

Fluoroquinolones constitute an important class of synthetic antimicrobial agents, which have been the objects of intensive study [1]. The history of the fluoroquinolones is directly related to nalidixic acid, which was the first quinolone found to present an antibacterial activity and was patented by Lescher et al. in 1962 [2]. It was discovered that the introduction of a fluorine atom at the C-6 position and a piperazyl group at the C-7 position conferred a broad and potent spectrum of antibacterial activity. Most notably sparfloxacin (SPF) (5-amino-1-cyclopropyl-7-[(3R,5S)3,5-dimethylpiperazin-1-yl]-6,8-difluoro-4-oxo-quinoline-3-carboxylic acid) and pefloxacin (PFLH) (1-ethyl-6-fluoro-7-(4-methylpiperazin-1-yl)-4-oxo-1,4-dihydroquinoline-3-carboxylic acid), both possess a broad spectrum of activity against various pathogenic microorganisms, in humans and animals, which are resistant to aminoglycosides, penicillin, cephalosporins, tetracyclines and other antibiotics. The bactericidal action results from

the inhibition of the enzymes topoisomerase II (DNA gyrase) and topoisomerase IV, required for bacterial DNA replication, transcription, repair, and recombination [3].

Metals have a structural role in many enzymes, which makes them natural targets in drug therapy and the development of enzyme inhibitors. The structural integrity and hence the function of the enzyme is influenced by the coordination of the metal with residues at/or outside the active site of the enzyme, which may block the substrate binding or interfere in the catalytic cycle. Alternatively, metal complexes targeting enzymes in the life cycle of the virus have been used as antivirals [4,5]. The human immunodeficiency virus, encodes three critical enzymes: a reverse transcriptase, an integrase and a protease.

Quinolone-metal complexes have been studied mainly for their antibacterial activity against diverse microorganisms [6–11] and in some cases, for their interaction with DNA [12,13], exemplifying the important role of metal ions for the mechanism of action of these drugs. Specifically,

Address for correspondence: Mohan N. Patel, Department of Chemistry, Sardar Patel University, Vallabh Vidyanagar–388 120, Gujarat, India.
E-mail: jeenen@gmail.com

(Received 17 February 2010; revised 08 April 2010; accepted 18 April 2010)

the *in-vitro* cytotoxicity of the complex [(chloro)(2,2'-bipyridine)(*N*-propyl-norfloxacinato)copper(II)] against two leukaemia cell lines, HL-60 (human acute myeloid leukaemia) and K562 (human chronic myeloid leukaemia in blast crisis), revealed an increased antiproliferative and necrotic effect, in comparison to the free ligand Hprnorf [14]. The copper complexes of phenanthroline and its derivatives are of great interest because they exhibit numerous biological activities such as antitumour [15], antibacterial [7], and antimicrobial [16]. Their intercalating properties [17] along with their function as artificial nucleases have also been reported [18–20].

In this work, we examined: (a) the synthesis and the structural characterisation of the Cu(II) complex of SPF/PFLH and neutral bidentate ligand; (b) the *in-vitro* antibacterial activity against five different microorganism; (c) its efficiency in performing DNA strand scission using herring sperm DNA and supercoiled pUC19 DNA; (d) its enzymatic activity against superoxide radical anion.

Experimental

Materials and reagents

All solvents, chemicals and reagents used were of analytical reagent grade and were used as such; double distilled water was used throughout. 2,2'-Bipyridylamine (A^1) was purchased from Lancaster (Morecambe, England). Sparfloxacin (SPF) and pefloxacin (PFLH) were generously supplied on demand by Bayer AG (Wuppertal, Germany). Cupric chloride dihydrate was purchased from E. Merck (India), Mumbai. Thiophene-2-carboxaldehyde (A^2), pyridine-2-carboxaldehyde (A^3), ethidium bromide, bromophenol blue, agarose and Luria broth were purchased from Himedia, India. Nicotinamide adenine dinucleotide reduced (NADH), nitro blue tetrazolium (NBT) and phenazin methosulphate (PMS) were purchased from Loba chemie PVT (Mumbai, India).

Instrumental measurement

Elemental analyses (C, H and N) of the synthesised complexes were performed with a model 240 Perkin Elmer elemental analyser. Room temperature magnetic measurement of the complexes was made using a Gouy magnetic balance (MA, USA). The Gouy tube (Mumbai, India) was calibrated using mercury(II) tetrathiocyanatocobaltate(II) as the calibrant ($\chi_g = 16.44 \times 10^{-6}$ cgs units at 20°C) [21]. Thermogravimetric analyses data were obtained with a model 5000/2960 SDTA, TA instrument (New Castle, DE, USA). The electronic spectra were recorded on a UV-160A UV-Vis spectrophotometer, Shimadzu (Kyoto, Japan). Infrared spectra were recorded on a FT-IR Shimadzu spectrophotometer as KBr pellets, in the range 4000–400 cm^{-1} . A minimal inhibitory concentration (MIC) study was carried out by means of a laminar air flow cabinet (Toshiba, Delhi). The FAB-mass spectra were recorded on a Jeol SX 102/Da-600 (MA, USA) mass spectrophotometer/data system using Argon/Xenon (6 kV, 10 mA) as the FAB

gas. The accelerating voltage was 10 kV and the spectra were recorded at room temperature. The photo quantisation of the gel after electrophoresis was done using the AlphaDigiDoc™ RT. Version V.4.0.0 PC-Image software (CA, USA).

Complex preparation

A methanolic solution of $\text{CuCl}_2 \cdot 2\text{H}_2\text{O}$ (1.5 mmol) was added to a methanolic solution of the neutral bidentate ligand (A^n) (1.5 mmol), followed by addition of a previously prepared solution of fluoroquinolone (1.5 mmol) in methanol in the presence of CH_3ONa (1.5 mmol). The pH of the solution was adjusted to ~6.2 pH using a dilute solution of CH_3ONa . The resulting solution was refluxed for 1 h on a steam bath, followed by concentrating it to half of its volume. The fine, amorphous green coloured product obtained was washed with ether/hexane and dried in a vacuum desiccator.

Spectrophotometric titration

Sample solutions were prepared by decomposing organic matter of the complex with an acid mixture and making it up to a total volume of 20 mL with double distilled water. Ten different sets of solutions were prepared by taking a fixed amount of complex solution (2 mL), 2 mL acetate buffer solution and varying aliquots of 0.001 M EDTA and making it up to total volume of 10 mL with double distilled water. The absorbance was measured at 745 nm using the buffer as a reference. The amount of copper was determined using the plot of absorbance against the volume of EDTA.

Biological evaluation

In-vitro antimicrobial screening

The antibacterial activity of the compounds was studied against *Escherichia coli* (*E. coli*), *Pseudomonas aeruginosa* (*P. aeruginosa*), *Bacillus subtilis* (*B. subtilis*), *Staphylococcus aureus* (*S. aureus*) and *Serratia marcescens* (*S. marcescens*). Screening was performed by determining the minimum inhibitory concentration (MIC) using Luria broth (LB) as a medium. The compounds were dissolved in sterile distilled water. Cultures for Gram (+ve) and Gram (-ve) were incubated at 37°C. A control test with no active ingredient was also performed [22]. The MIC was determined using two-fold serial dilutions in liquid media containing a 0.2–3,500 μM variation of the test compound concentration. A pre-culture of bacteria was grown in LB overnight at the optimal temperature for each species. We monitored bacterial growth by measuring the turbidity of the culture after 18 hours. If a certain concentration of a compound inhibited the bacterial growth, half the concentration of the compound was then tested. This procedure was carried on until a concentration was reached where the bacteria grew normally. The lowest concentration that inhibited bacterial growth was determined as the MIC value. All equipment and culture media used were sterile.

DNA interaction study

To evaluate the DNA-interaction properties of the synthesised analogues, a UV-Vis absorbance titration experiment, viscosity titration and gel electrophoresis photo quantisation techniques were used with herring sperm and pUC19 DNA and were compared.

Absorbance titration experiment

The binding of DNA via the intercalation mode usually results in hypochromism and bathchromism [22–26], because the intercalation mode involves a strong stacking interaction between an aromatic chromophore and the DNA base pair [27]. With the selection of the appropriate absorbance peak, spectrophotometric wavelength scans of each Cu(II) complexes were performed. After addition of the equivalent amount of DNA to the reference cell, incubation for 10 minutes at room temperature and followed by the absorption measurement. This was specifically done to enable the direct comparison between the assays that was required to interpret the results obtained. The intrinsic binding constant, K_b was determined by making it the subject of the following equation [28]:

$$[\text{DNA}]/(\varepsilon_a - \varepsilon_f) = [\text{DNA}]/(\varepsilon_b - \varepsilon_f) + 1/K_b(\varepsilon_b - \varepsilon_f)$$

where, [DNA] is the concentration of DNA in terms of nucleotide phosphate, [NP] is the apparent absorption coefficients and ε_a , ε_f and ε_b correspond to $A_{\text{obs.}}/[M]$, the extinction coefficient for the free copper complex and the free copper complex in the fully bound form, respectively and K_b is the ratio of the slope to the y intercept.

Viscosity titration

The viscosity measurement is regarded as a reliable tool to determine the binding mode in a solution state in the absence of the crystallographic structural data and the NMR data [29]. The viscometric titrations were performed using an Ubbelohde viscometer (Cannon, PA, USA) immersed in a thermostatic bath maintained at $27^\circ\text{C} \pm 0.1^\circ\text{C}$. The flow time was measured with a digital stopwatch, each sample was measured in triplicate and an average flow time was calculated. The data are presented as $(\eta/\eta_0)^{1/3}$ versus [complex]/[DNA], where η is the viscosity of DNA in the presence of complex and η_0 is the viscosity of the DNA alone. The viscosity values

were calculated from the observed flow time of the DNA-containing solutions (t) corrected for that of the buffer alone (t_0), using the following equation [30];

$$\eta = (t - t_0)$$

Gel electrophoresis; photo quantisation technique

For the gel electrophoresis experiments; a total volume of 15 μL containing 300 $\mu\text{g}/\text{mL}$ of pUC19 DNA in TE buffer (10 mM Tris, 1 mM EDTA, pH 8) was treated with different complexes (200 μM) and the mixture was incubated for 24 h at 37°C . The samples were then analysed on the basis of their charge and size difference on a 1% agarose gel bed consisting of 0.5 $\mu\text{g}/\text{mL}$ of ethidium bromide at 50 V, after quenching the reaction with 5 μL loading buffer (40% sucrose, 0.2% bromophenol blue). The whole bed was immersed in 1X TAE buffer (0.04 M Tris-Acetate, pH 8, 0.001 M EDTA). The Bands were visualised using UV light, then photographed followed by an estimation of the intensity of the DNA bands using the AlphaDigiDoc™ RT. Version V.4.0.0 PC-Image software gel documentation system.

SOD like activity: decomposition of reactive oxygen species

This used a non-enzymatic system made up of 30 μM PMS, 79 μM NADH, 75 μM NBT and phosphate buffer (pH 7.8) to produce the superoxide anion ($\text{O}_2^{\cdot-}$). The scavenging rate of $\text{O}_2^{\cdot-}$ was determined by monitoring the reduction in the rate of transformation of NBT to monoformazan dye under the influence of 0.25 to 5.0 μM of tested compound [29]. The reactions were monitored at 560 nm with a UV-Vis Spectrophotometer and the rate of absorption change was determined. The percentage inhibition of the NBT reduction was calculated using following equation [31]:

$$\% \text{ inhibition of NBT reduction} = (1 - k'/k) \times 100\%$$

where, k' and k present the slopes of the straight line of absorbance values as a function of time, in the presence and absence of SOD mimic compound, respectively. The IC_{50} value for the complex was determined by plotting the graph of percentage of inhibiting NBT reduction against the increase in the concentration of the complex. The concentration of the complex which caused 50% inhibition of NBT reduction was reported as the IC_{50} .

Table 1. Physicochemical parameters and elemental details of the complexes.

Empirical formula for complexes	Elemental analysis% required (found)				Mp $^\circ\text{C}$	% Yield	μ_{eff} BM	λ_{max} nm	Formula weight (g/mol)
	C	H	N	Cu					
$\text{C}_{29}\text{H}_{40}\text{ClCuF}_2\text{N}_7\text{O}_8$ (1)	46.34(46.23)	5.36(5.85)	13.04(12.95)	8.45(8.39)	>300	75.44	1.77	668	750.19
$\text{C}_{24}\text{H}_{35}\text{ClCuF}_2\text{N}_4\text{O}_9\text{S}$ (2)	41.62(41.58)	5.09(5.01)	8.09(8.16)	9.17(9.19)	294	87.66	1.89	662	691.11
$\text{C}_{25}\text{H}_{36}\text{ClCuF}_2\text{N}_5\text{O}_9$ (3)	43.67(43.74)	5.28(5.19)	10.19(10.02)	9.24(9.67)	>300	87.53	1.81	671	686.15
$\text{C}_{27}\text{H}_{38}\text{ClCuFN}_6\text{O}_8$ (4)	46.82(46.83)	5.53(5.54)	12.13(12.12)	9.17(9.16)	298	78.32	1.74	659	691.17
$\text{C}_{22}\text{H}_{34}\text{ClCuFN}_3\text{O}_9\text{S}$ (5)	41.64(41.59)	5.4(5.38)	6.62(6.66)	10.01(9.97)	276	81.04	1.83	663	633.1
$\text{C}_{23}\text{H}_{34}\text{ClCuFN}_4\text{O}_9$ (6)	43.95(43.92)	5.45(5.42)	8.91(8.93)	10.11(10.12)	292	77.97	1.79	657	627.13

Results and discussion

Characterisation of complexes

The FT-IR, UV-Vis spectroscopy, magnetic measurement and FAB-MS techniques were used to evaluate the structure of the complexes. The physico-chemical parameters and microanalysis data (Table 1) were in good agreement with the proposed structure (Figure 1).

Spectrophotometric titration

The amount of copper was determined by a spectrophotometric titration technique [32,33]. The calculated results from the equivalent endpoint (Figure 2) revealed the metallic content of the complex (Table 2) (Supplementary 2: The spectrophotometric titration curves for the equivalent endpoint determination of the complexes).

IR spectroscopy

The IR spectra of the Cu(II) complexes showed major changes as compared to the free ligands (Table 3). The absorption bands observed in the case of pefloxacin at 1632 and 1308 cm^{-1} were assigned to the $\nu(\text{COO})_{\text{assy}}$

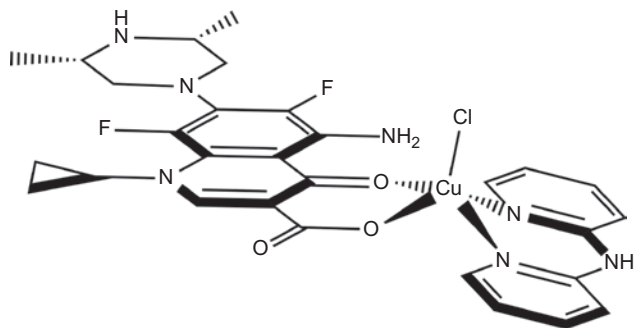


Figure 1. Structure of the title complex $[\text{Cu}(\text{SPF})(\text{A}^1)\text{Cl}] \cdot 5\text{H}_2\text{O}$ [1].

and the $\nu(\text{COO})_{\text{sym}}$ respectively, whereas the bands for same functionality in the case of sparfloxacin appeared at 1620 and 1332 cm^{-1} . In the complexes, these bands were observed at ~ 1578 and ~ 1345 cm^{-1} . The frequency separation ($\Delta\nu = \nu\text{COO}_{\text{assy}} - \nu\text{COO}_{\text{sym}}$) in the investigated complexes was ~ 233 cm^{-1} , suggesting a unidentate nature for the carboxylato group [34–36]. The sharp band for quinolone at ~ 3522 cm^{-1} was due to hydrogen bonding [37]; which contributes to ionic resonance structure and the peak observed was from a free hydroxyl stretching vibration. This band completely vanished in the spectra of the complexes, which indicated deprotonation of the carboxylic proton. The

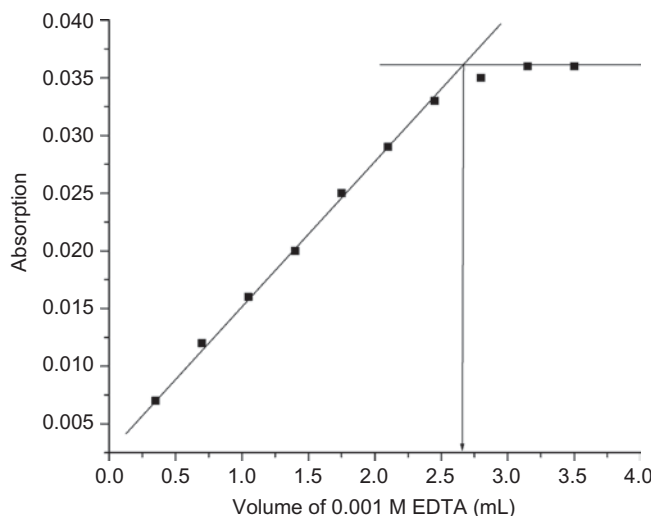


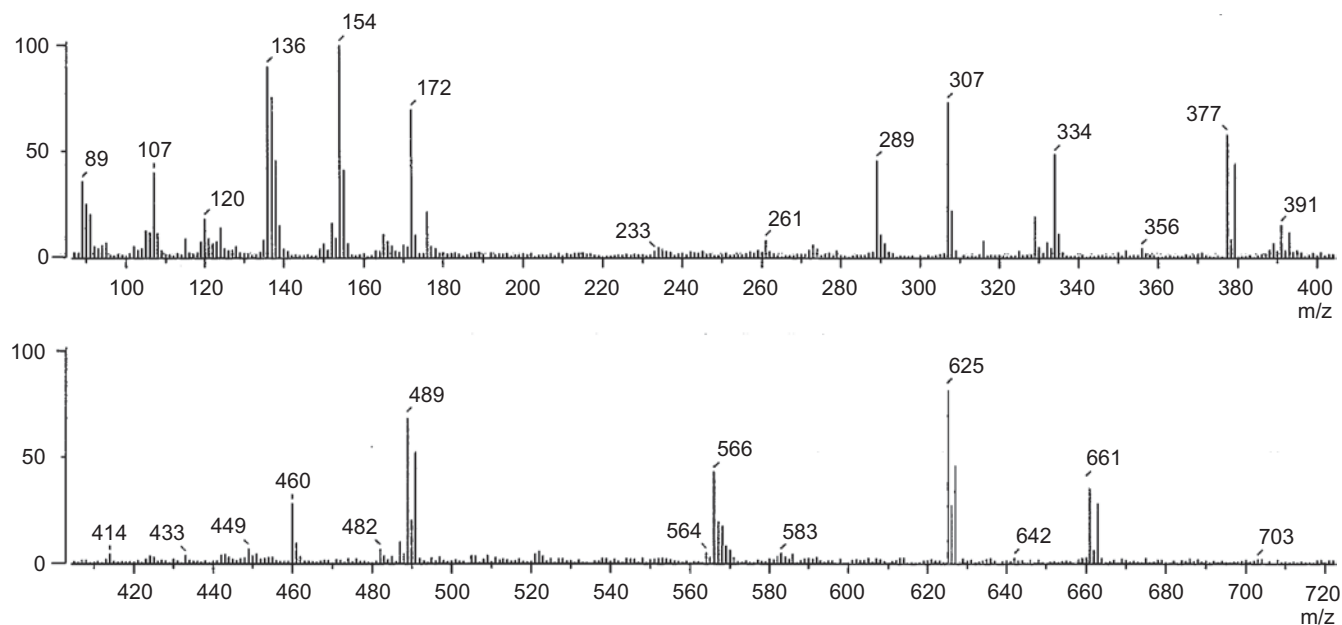
Figure 2. Experimental curve from the spectrophotometric determination of metal content of 20.12 mg complex $[\text{Cu}(\text{SPF})(\text{A}^1)\text{Cl}] \cdot 5\text{H}_2\text{O}$ dissolved in 20 ml of DD water by EDTA.

Table 2. Spectrophotometric titration data for the complexes.

Volume of 0.001 M EDTA (mL)	Absorption at 745 nm					
	(1)	(2)	(3)	(4)	(5)	(6)
0.35	0.007	0.006	0.004	0.01	0.006	0.008
0.7	0.012	0.009	0.007	0.014	0.011	0.012
1.05	0.016	0.014	0.011	0.018	0.016	0.016
1.4	0.02	0.017	0.014	0.021	0.02	0.02
1.75	0.025	0.02	0.018	0.024	0.026	0.024
2.1	0.029	0.024	0.021	0.027	0.029	0.028
2.45	0.033	0.028	0.025	0.032	0.034	0.032
2.8	0.035	0.031	0.028	0.035	0.036	0.035
3.15	0.036	0.033	0.03	0.036	0.036	0.036
3.5	0.036	0.033	0.03	0.036	0.036	0.036
Amount of complex dissolved in 20 ml (g)	0.02012	0.02064	0.02008	0.01989	0.01642	0.01792
Equivalents volume of 0.001 M EDTA (mL)	2.667	2.98556	2.9234	2.866	2.594	2.844
Equivalent Concentration of EDTA at end point (M)	0.0002667	0.000298556	0.00029234	0.0002866	0.0002594	0.0002844
Amount of Cu in 2 mL (g)	0.000169477	0.00018972	0.00018577	0.000182123	0.00016484	0.000180725
Amount of Cu in 20 mL (g)	0.001694772	0.001897204	0.0018577	0.001821228	0.00164838	0.001807248
% Cu experimental	8.42	9.19	9.25	9.16	10.04	10.09
% Cu theoretically	8.45	9.17	9.24	9.17	10.01	10.11

Table 3. Characteristic absorptions bands of IR spectra of the complexes and drugs (cm⁻¹).

Comp	$\nu(\text{C=O})_{\text{pyridone}}$	$\nu(\text{H-O})_{\text{Carboxyl}}$	$\nu(\text{COO})_{\text{asy}}$	$\nu(\text{COO})_{\text{sym}}$	$\Delta\nu$	$\nu(\text{M-N})$	$\nu(\text{M-O})$	$\nu(\text{M-S})$
SPF	1728	3526	1620	1332	288	-	-	-
PFLH	1716	3518	1632	1308	324	-	-	-
1	1623	-	1585	1346	236	536	518	-
2	1625	-	1581	1351	225	534	514	432
3	1621	-	1579	1342	232	546	515	-
4	1627	-	1583	1344	239	539	521	-
5	1624	-	1589	1355	234	537	512	436
6	1617	-	1577	1342	235	544	517	-

Figure 3. The FAB-mass spectrum of $[\text{Cu}(\text{SPF})(\text{A}^1)\text{Cl}]\cdot 5\text{H}_2\text{O}$ at an accelerating voltage of 10kV.

$\nu(\text{C=O})$ stretching vibration band for pefloxacin and sparfloxacin appeared at 1716 and 1728 cm⁻¹, respectively. While in the complexes this band was shifted at ~1625 cm⁻¹; this shift in band towards lower energy suggested that coordination occurs through the pyridone oxygen atom [38]. These data are further supported by the $\nu(\text{M-O})$ [39] which appeared at ~517 cm⁻¹ for the complexes. The band at ~536 cm⁻¹ observed in the case of the complexes suggested the NN donating nature of the 2,2'-bipyridylamine [40].

Electronic spectra and magnetic data

A visible emission spectra of the copper(II) complexes i.e. d^9 system were recorded in DMSO. Complexes exhibited the only broad λ_{max} at ~663 nm, which were attributed to a $d-d$ transition for the Cu(II) atom in a distorted square pyramidal environment [41,42]. The possibility of trigonal bipyramidal geometry at the metal centre was ruled out because the pattern of a $\lambda_{\text{max}} > 800$ nm, along with a shoulder at ~660 nm was not observed in the case of the synthesised complexes [43,44].

The magnetic moments measurement for any geometry in the copper(II) complexes generally resulted in 1.8 BM, which is very close to a spin-only value i.e. 1.73 BM.

The observed values in our case were very close to the spin-only values (Table 1) for the single unpaired electron, this confirmed the copper being in a +2 state with a d^9 configuration ($t_{2g}^6 e_g^3$) [45,46].

Thermogravimetric analysis

The interpretation of the thermogravimetric curves of the synthesised complexes showed that the complexes possessed five molecules of water of crystallisation, which were liberated between 50–120°C [47]. The weight loss between 180–430°C and 450–690°C corresponded to the decomposition of the neutral bidentate ligand and fluoroquinolone respectively, leaving behind CuO as a residue.

FAB-mass spectra

The FAB-mass spectrum of the representative complex, that is $[\text{Cu}(\text{SPF})(\text{A}^1)\text{Cl}]\cdot 5\text{H}_2\text{O}$, obtained using *m*-nitro benzyl alcohol as matrix is shown in Figure 3. The peaks at the 136, 137, 154, 289 and 307 m/z values were due to the usage of matrix. The peak at 661 m/z value were assigned to the molecular weight of the complex molecule associated with one H⁺ ion in the absence of crystalline water. There also existed several peaks at 489, 625 and 377 m/z values which also showed a doublet

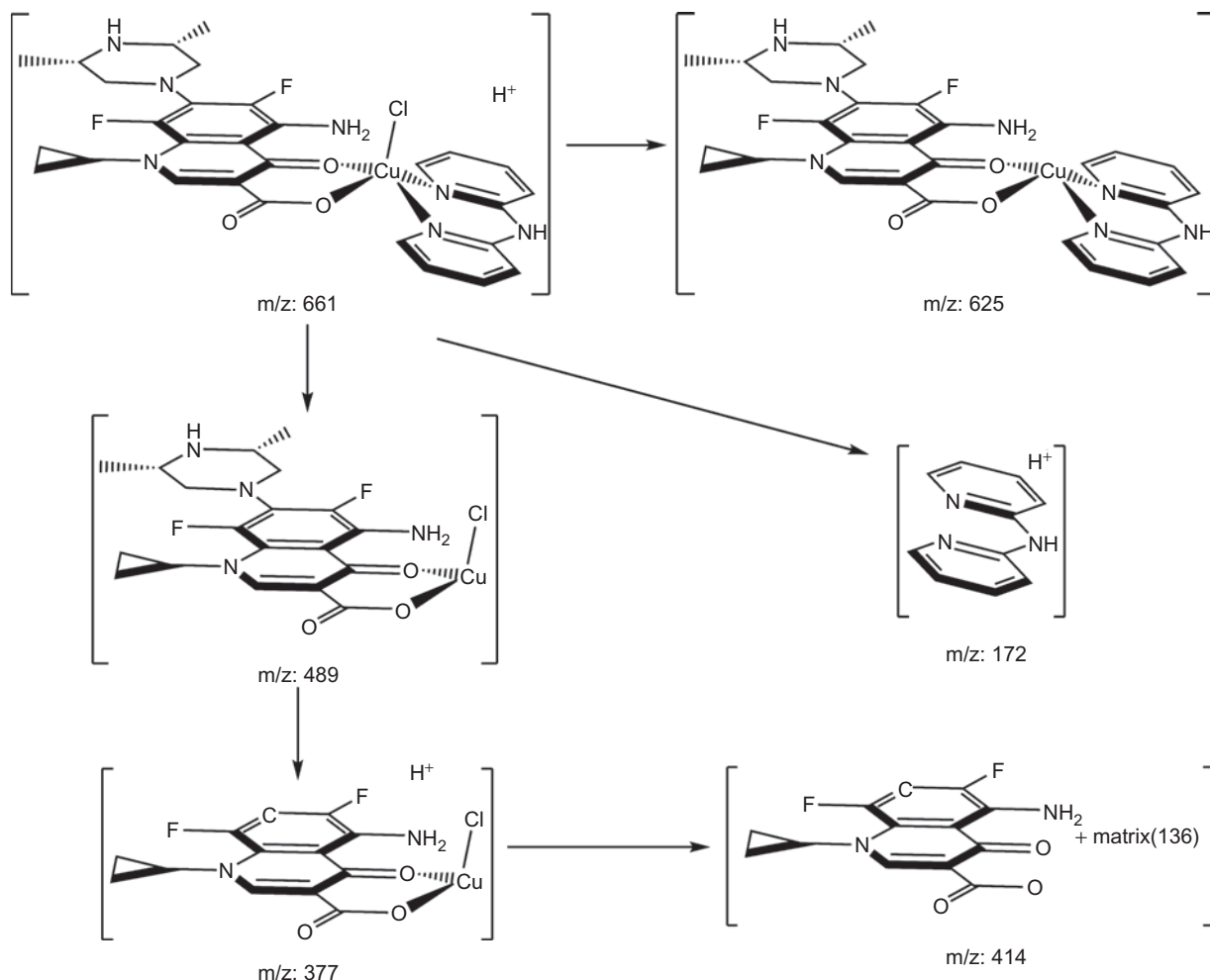


Figure 4. Proposed fragmentation pattern for $[\text{Cu}(\text{SPF})(\text{A}^1)\text{Cl}]\cdot 5\text{H}_2\text{O}$ complex.

pattern as if the compound had one Cl atom, hence it could be concluded that these fragments consisted of one Cl atom [48]. Several other fragments at 172, 414 etc. m/z values were observed and could be attributed to other fragments associated with H^+ ions (Figure 4).

Biological evaluation

In-vitro antimicrobial screening

The synthesised complexes, ligands, drugs and metal salts were checked for their *in-vitro* antibacterial activity in terms of their minimum inhibitory concentration (MIC) against bacterial strains such as *E. coli*, *P. aeruginosa*, *S. aureus*, *B. Subtilis*, and *S. marcescens* (Table 4). The following conclusions were drawn from the antibacterial data:

1. *S. aureus*: Complexes 3, 4 and 6 were more active compare to the other complexes and drugs.
2. *B. subtilis*: Except for complex 6, all were more potent than drugs.
3. *S. marcescens*: Except for complex 4, all had moderate to poor activity against this species.
4. *P. aeruginosa*: Complex 4 and 6 were more active than both the drugs employed, whereas the others had moderate to poor activity.

5. *E. coli*: Complex 4 was the only active complex compared to the drugs employed.

From the data, it was concluded that complex 4 was more active than others. In addition, there was a major change in activity of pefloxacin compared to sparfloxacin. From this data it could also be concluded that no particular pattern for the ligands or drug was observed. But whatever increase in antimicrobial activity was observed may be studied under the following five principles [49–52]:

- (I) The chelate effect, i.e. ligands that are bound to metal ions in a bidentate fashion, such as the quinolones and phenanthroline, bipyridine or bipyridylamine show higher antimicrobial efficiency towards complexes with N-donor ligands.
- (II) The nature of the ligands.
- (III) The total charge of the complex; generally the antimicrobial efficiency decreases in the order cationic > neutral > anionic complex.
- (IV) The nature of the ion neutralising the ionic complex.
- (V) The nuclearity of the metal centre in the complex; dinuclear centres are usually more active than mononuclear ones.

Table 4. MIC in terms of μM .

Compounds	Gram positive		Gram negative		
	<i>S. aureus</i>	<i>B. subtilis</i>	<i>S. marcescens</i>	<i>P. aeruginosa</i>	<i>E. coli</i>
$\text{CuCl}_2 \cdot 2\text{H}_2\text{O}$	2698	2815	2756	2404	3402
Sparfloxacin(SPF)	1.3	2.0	1.5	1.5	1.3
Pefloxacin(PFLH)	2.1	2.4	5.1	5.7	2.7
A ¹	3212	3271	3212	3183	3154
A ²	>10000	>10000	>10000	>10000	>10000
A ³	3821	3414	3333	2902	3739
$[\text{Cu}(\text{SPF})(\text{A}^1)\text{Cl}].5\text{H}_2\text{O}$ (1)	1.8	1.8	5.5	2.7	2.7
$[\text{Cu}(\text{SPF})(\text{A}^2)\text{Cl}].5\text{H}_2\text{O}$ (2)	1.7	1.7	10.5	6.2	6.1
$[\text{Cu}(\text{SPF})(\text{A}^3)\text{Cl}].5\text{H}_2\text{O}$ (3)	0.9	1.2	4.4	3.5	13.9
$[\text{Cu}(\text{PFL})(\text{A}^1)\text{Cl}].5\text{H}_2\text{O}$ (4)	0.9	1.2	0.9	0.3	0.3
$[\text{Cu}(\text{PFL})(\text{A}^2)\text{Cl}].5\text{H}_2\text{O}$ (5)	1.6	1.6	1.9	1.7	1.7
$[\text{Cu}(\text{PFL})(\text{A}^3)\text{Cl}].5\text{H}_2\text{O}$ (6)	0.9	3.5	2.7	0.9	3.5

Thus, the first two factors may be considered for the increase in the activity i.e. the chelate effect.

DNA interaction study

Absorption titration experiment

The quinolone metal complex can bind to DNA via three distinct binding sites namely, groove-binding, binding to the phosphate group and intercalation [53]. These behaviours are of great importance with regard to the relevant biological role of quinolone antibiotics in the body [54,55]. The changes observed in the UV spectra of the complexes after mixing it with DNA (either the increase of the intensity or the shift of the wavelength) indicated that the interaction of the complexes with DNA takes place by a direct formation of a new complex with the double-helical DNA [56]. The extent of the binding strength of the complexes was quantitatively determined by calculating the intrinsic binding constants K_b of the complexes by monitoring the change in absorbance at various concentration of DNA (Figure 5). From the plot of $[\text{DNA}]/(\epsilon_a - \epsilon_f)$ versus $[\text{DNA}]$, (Inset figure 5) the K_b value of complexes were determined and were found to be in the range of $1.009\text{--}0.721 \times 10^4$ (Table 5), which is much lower than that of the classical intercalator (ethidium bromide), thus there is a possibility of intercalation of the complexes. Therefore, the results indicated that the complexes may first bind with the phosphate group of DNA, neutralise the negative charge of the DNA phosphate group, and cause the contraction and conformational change to DNA.

Viscosity titration

Viscosity measurement can be regarded as a reliable tool in the absence of crystallographic and NMR data [57]. The intercalation of a molecule into DNA could result in lengthening, unwinding and stiffening of the helix and is usually accompany by increases in solution viscosity [58,59]. In this case an increase in viscosity was observed, hence the complexes were bound to DNA via an intercalation mode and out of all the complexes, complex 1 interacted more strongly compare to the others (Figure 6).

Table 5. The binding constants (K_b) and IC_{50} values of the complexes.

Complexes	K_b (M^{-1})	IC_{50} (μM)
$[\text{Cu}(\text{SPF})(\text{A}^1)\text{Cl}].5\text{H}_2\text{O}$ (1)	0.725×10^4	0.862
$[\text{Cu}(\text{SPF})(\text{A}^2)\text{Cl}].5\text{H}_2\text{O}$ (2)	0.793×10^4	1.058
$[\text{Cu}(\text{SPF})(\text{A}^3)\text{Cl}].5\text{H}_2\text{O}$ (3)	1.009×10^4	1.354
$[\text{Cu}(\text{PFL})(\text{A}^1)\text{Cl}].5\text{H}_2\text{O}$ (4)	0.689×10^4	0.781
$[\text{Cu}(\text{PFL})(\text{A}^2)\text{Cl}].5\text{H}_2\text{O}$ (5)	0.721×10^4	1.139
$[\text{Cu}(\text{PFL})(\text{A}^3)\text{Cl}].5\text{H}_2\text{O}$ (6)	9.873×10^4	1.296

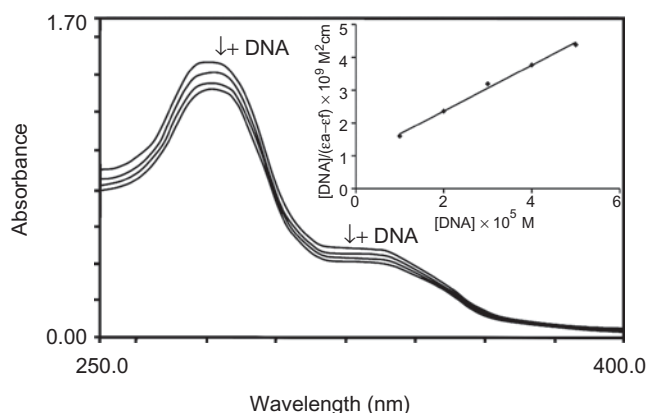


Figure 5. Electronic absorption spectra of $[\text{Cu}(\text{SPF})(\text{A}^1)\text{Cl}].5\text{H}_2\text{O}$ in phosphate buffer ($\text{Na}_2\text{HPO}_4/\text{NaH}_2\text{PO}_4$, pH 7.2) in the absence and presence of increasing amount of DNA. The $[\text{Cu}]$ complex = $10 \mu\text{M}$; $[\text{DNA}] = 0\text{--}150 \mu\text{M}$. The incubation period is 30 min at 37°C . Inset: Plot of $[\text{DNA}]/(\epsilon_a - \epsilon_f)$ vs. $[\text{DNA}]$. Arrow shows the absorbance change upon increasing DNA concentrations.

Gel electrophoresis; photo quantisation technique

Transition metal complex mediated DNA cleavage is of central interest [60,61]. When plasmid DNA was subjected to electrophoresis after the interaction, illumination of the gel revealed (Figure 7) that the fastest migration was observed for the super coiled (SC) Form I, whereas the slowest moving form was the open circular (OC) Form II and the intermediate moving form was the linear (LC) Form III (generated on cleavage of the open circular form). The plasmid cleavage data showed that complexes 1 and 6 had the maximum cleavage ability compared to all the synthesised complexes (Table 6).

The different DNA-cleavage efficiency of the complexes, metal salt and drugs was due to the difference in binding affinity of the complexes to the DNA and the structural dissimilarities of the ligands.

SOD like activity: decomposition of the reactive oxygen species

The NADH/PMS/NBT system was used to generate the superoxide radical artificially in order to check SOD like behaviour of the complexes. The percentage inhibition of formazan formation at various concentrations of the complexes as a function of time was determined by measuring the absorbance at 560 nm and this was plotted to give a straight line obeying the equation $Y = mX + C$ (Figure 8); with an increase in the concentration of tested complexes a decrease in the slope (m) was observed. The percentage inhibition of the reduction rate of nitro blue tetrazolium (NBT) was plotted against the concentration of the complex to obtain the IC_{50} value (Figure 9). The compounds exhibited a SOD-like activity at biological pH with their IC_{50} values ranging from 0.781 to 1.354 μM (Table 5). The best IC_{50} value among the synthesised complexes was observed for complex 4. The higher IC_{50} can only be accredited to the vacant coordination site facilitating the binding of the superoxide anion, electrons of the aromatic ligands that stabilise the $Cu-O_2^-$ interaction and not only to the partial dissociation of the complex in solution. Plots for determination of the IC_{50}

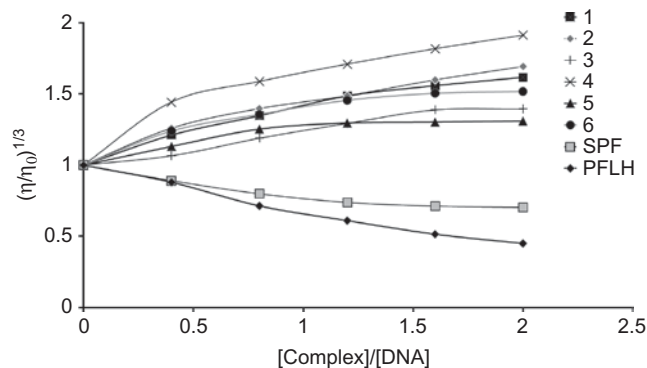


Figure 6. Effect on relative viscosity of DNA under the influence of increasing amount of complexes at $27^{\circ}C \pm 0.1^{\circ}C$ in phosphate buffer (Na_2HPO_4/NaH_2PO_4 , pH 7.2).

values for the other complexes are in the supplementary material (Supplementary 3: Plots for determination of IC_{50} of complexes).

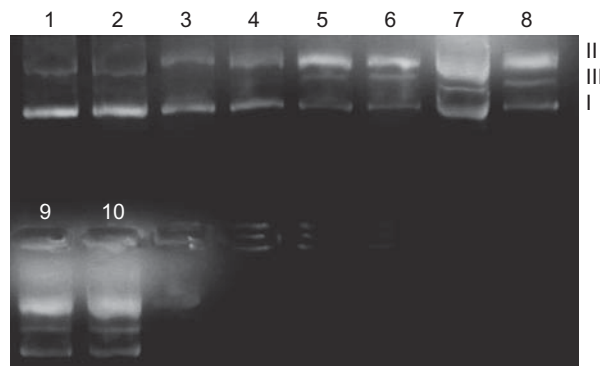


Figure 7. Photogenic view of cleavage of pUC19 DNA (300 $\mu g/mL$) with series of copper(II) complexes (200 μM) using 1% agarose gel containing 0.5 $\mu g/mL$ ethidium bromide. All reactions were incubated in TE buffer (pH 8) in a final volume of 15 μL , for 24 h. at $37^{\circ}C$. Lane 1, DNA control; Lane 2, $CuCl_2 \cdot 2H_2O$; Lane 3, Sparfloxacin; Lane 4, Pefloxacin; Lane 5, $[Cu(SPF)(A^1)Cl] \cdot 5H_2O$; Lane 6, $[Cu(SPF)(A^2)Cl] \cdot 5H_2O$; Lane 7, $[Cu(SPF)(A^3)Cl] \cdot 5H_2O$; Lane 8, $[Cu(PFL)(A^1)Cl] \cdot 5H_2O$; Lane 9, $[Cu(PFL)(A^2)Cl] \cdot 5H_2O$; Lane 10, $[Cu(PFL)(A^3)Cl] \cdot 5H_2O$.

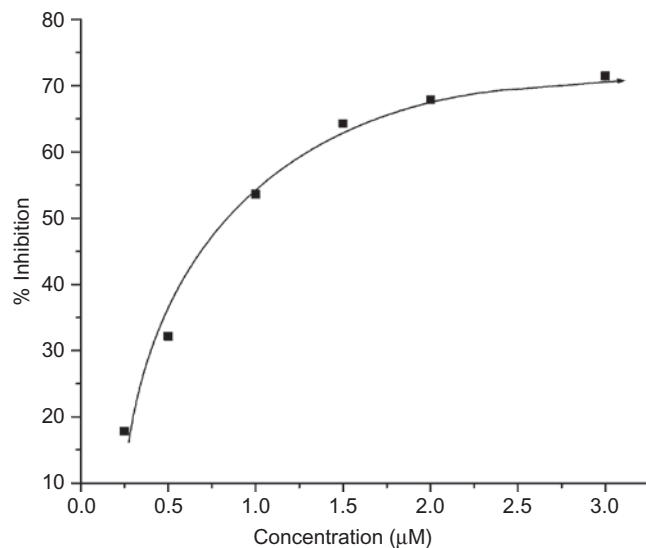


Figure 9. Plot of percentage of inhibiting NBT reduction with an increase in the concentration of complex 1.

Table 6. Complex mediated DNA cleavage data by gel electrophoresis.

Lane No	Compound	Form ISC	Form IIOC	Form IIIIC
1	Control	83	17	-
2	$CuCl_2 \cdot 2H_2O$	82	18	-
3	Sparfloxacin	58	42	-
4	Pefloxacin	54	46	-
5	$[Cu(SPF)(A^1)Cl] \cdot 5H_2O$ (1)	11	75	14
6	$[Cu(SPF)(A^2)Cl] \cdot 5H_2O$ (2)	14	65	21
7	$[Cu(SPF)(A^3)Cl] \cdot 5H_2O$ (3)	24	63	13
8	$[Cu(PFL)(A^1)Cl] \cdot 5H_2O$ (4)	19	69	12
9	$[Cu(PFL)(A^2)Cl] \cdot 5H_2O$ (5)	12	77	11
10	$[Cu(PFL)(A^3)Cl] \cdot 5H_2O$ (6)	11	71	18

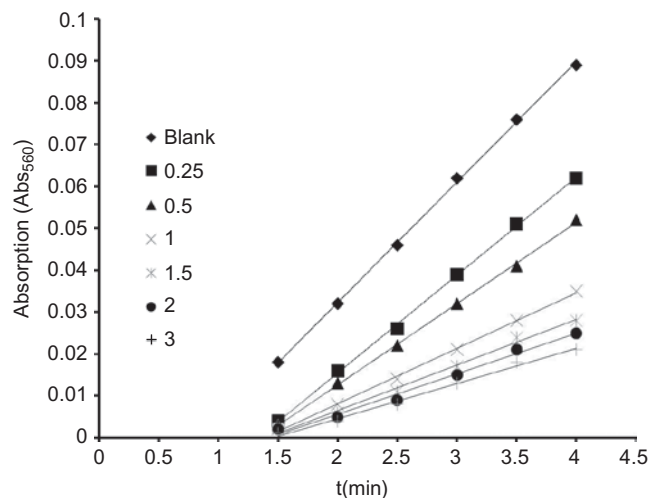


Figure 8. Absorbance values (Abs_{560}) as a function of time (t) plotted for varying concentration of complex 1 from 0.25 μ M to 3 μ M for produced a good straight line are observed.

Conclusions

The complexes derived from NN-diphenylamine were found to be much more active compared to the other complexes. While comparing the MIC data of the complexes and drugs, complex 4 prepared from the pefloxacin (PFLH) and A^1 gave good results for all the microorganisms. The reason behind this increase in potency of the drug is its coordination with a metal ion. From the viscosity data of the complexes; it is clear that all complexes showed classical intercalative modes of binding, whereas complex 4 was bound more strongly than the others. The electronic absorption data were in good accordance with the viscosity titration curves. The DNA cleavage study of pUC19 showed that all the complexes had high cleavage ability compared to the metal salt and drug. Upon determination of the antioxidant activity in the NBT/NADH/PMS system, complex 4 showed the highest scavenging ability for the oxygen radical. Our group is currently examining a range of biological interactions that these metallo-intercalators may undergo inside the cell in order to understand their biochemistry and mechanism of action in a better way.

Acknowledgements

The authors would like to thank the Head, Department of Chemistry, Sardar Patel University, India for making it convenient to work in laboratory and the UGC for providing financial support under the scheme "UGC Research Fellowship in Science for Meritorious Students".

Declaration of interest

The authors report no conflicts of interest. The authors alone are responsible for the content and writing of the paper.

References

- de Souza MVN, de Almeida MV, da Silva AD, Couri MRC. Biological activity and synthetic methodologies for the preparation of fluoroquinolones, a class of potent antibacterial agents. *Curr Med Chem* 2003;10:21-39.
- Lescher GY, Froelich ED, Gruet MD, Bailey JH, Brundage RP. 1, 8-Naphthyridine derivatives. A new class of chemotherapeutic agents. *J Med Pharm Chem* 1962;5:1063-1068.
- Appelbaum PC, Hunter PA. The fluoroquinolone antibacterials: past, present and future perspectives. *Int J Antimicrob Agents* 2000;16:5-15.
- La Femina RL. Requirement of active human immunodeficiency virus type 1 Integrase enzyme for productive infection of human T-lymphoid Cells. *J Virol* 1992;66:7414-7419.
- Moore PS, Jones CJ, Mahmood N, Evans IG, Goff M, Cooper R, Hay AJ. Anti-(human immunodeficiency virus) activity of polyoxotungstates and their inhibition of human immunodeficiency virus reverse transcriptase. *Biochem J* 1995;307:129-134.
- Turel I, Golobic A, Klavzar A, Pihlar B, Buglyo P, Tolis E, Rehder D, Sepcic K. Interactions of oxovanadium(IV) and the quinolone family member--ciprofloxacin. *J Inorg Biochem* 2003;95:199-207.
- Saha DK, Sandbhor U, Shirisha K, Padhye S, Deobagkar D, Anson CE, Powell AK. A novel mixed-ligand antimycobacterial dimeric copper complex of ciprofloxacin and phenanthroline. *Bioorg Med Chem Lett* 2004;14:3027-3032.
- Ruiz M, Perello L, Ortiz R, Castineiras A, Maichle-Mossmar C, Canton E. Synthesis, characterization, and crystal structure of $[Cu(cinoxacin)_2] \cdot 2H_2O$ complex: A square-planar CuO_4 chromophore. Antibacterial studies. *J Inorg Biochem* 1995;59:801-810.
- Lopez-Gresa MP, Ortiz R, Perello L, Latorre J, Liu-Gonzalez M, Garcia-Granda S, Perez-Priede M, Canton E. Interactions of metal ions with two quinolone antimicrobial agents (cinoxacin and ciprofloxacin): Spectroscopic and X-ray structural characterization. Antibacterial studies. *J Inorg Biochem* 2002;92:65-74.
- Ruiz M, Perello L, Server-Carrio J, Ortiz R, Garcia-Granda S, Diaz MR, Canton E. Cinoxacin complexes with divalent metal ions. Spectroscopic characterization. Crystal structure of a new dinuclear Cd(II) complex having two chelate-bridging carboxylate groups. Antibacterial studies. *J Inorg Biochem* 1998;69:231-239.
- Turel I, Golic L, Bukovec P, Gubina M. Antibacterial tests of bismuth(III)-quinolone (ciprofloxacin, cf) compounds against *Helicobacter pylori* and some other bacteria. Crystal structure of $(C_6H_5)_2[Bi_2Cl_{10}] \cdot 4H_2O$. *J Inorg Biochem* 1998;71:53-60.
- Jimenez-Garrido N, Perello L, Ortiz R, Alzuet G, Gonzalez-Alvarez M, Canton E, Liu-Gonzalez M, Garcia-Granda S, Perez-Priede M. Antibacterial studies, DNA oxidative cleavage, and crystal structures of Cu(II) and Co(II) complexes with two quinolone family members, ciprofloxacin, and enoxacin. *J Inorg Biochem* 2005;99:677-689.
- Drevensek P, Turel I, Poklar UN. Influence of copper(II) and magnesium(II) ions on the ciprofloxacin binding to DNA. *J Inorg Biochem* 2003;96:407-415.
- Efthimiadou EK, Thomadaki H, Sanakis Y, Raptopoulou CP, Katsaros N, Scorilas A, Karaliota A, Psomas G. Structure and biological properties of the copper(II) complex with the quinolone antibacterial drug N-propyl-norfloxacin and 2,2'-bipyridine. *J Inorg Biochem* 2007;101:64-73.
- Ranford JD, Sadler PJ, Tocher DA. Cytotoxicity and antiviral activity of transition-metal salicylate complexes and crystal structure of bis(diisopropylsalicylate)(1,10-phenanthroline)copper(II). *J Chem Soc, Dalton Trans* 1993;22:3393-3399.
- Zoroddu MA, Zanetti S, Pogni R, Basosi R. An electron spin resonance study and antimicrobial activity of copper(II)-phenanthroline complexes. *J Inorg Biochem* 1996;63:291-300.
- Erkkila KE, Odom DT, Barton JK. Recognition and reaction of metallointercalators with DNA. *Chem Rev* 1999;99:2777-2796.
- Sigman DS. Chemical nucleases. *Biochemistry* 1990;29:9097-9105.

19. Sigman DS, Mazumder A, Perrin DM. Chemical nucleases. *Chem Rev* 1993;93:2295–2316.
20. Pogozelski WK, Tullius TD. Oxidative strand scission of nucleic acids: Routes initiated by hydrogen abstraction from the sugar moiety. *Chem Rev* 1998;98:1089–1108.
21. Henderson LJ Jr., Fronczek FR, Cherry WR. Selective perturbation of ligand field excited states in polypyridine ruthenium(II) complexes. *J Am Chem Soc* 1984;106:5876–5879.
22. Alexious M, Tsivikas I, Dendrinou-Samara C, Pantazaki AA, Trikalitis P, Lalioti N, Kyriakidis DA, Kessissoglou DP. High nuclearity nickel compounds with three, four or five metal atoms showing antibacterial activity. *J Inorg Biochem* 2003;93:256–264.
23. Mudasir, Yoshioka N, Inoue H. DNA Binding of iron(II) mixed-ligand complexes containing 1,10-phenanthroline and 4,7-diphenyl-1,10-phenanthroline. *J Inorg Biochem* 1999;77:239–247.
24. Fin L, Yang P. Synthesis and DNA binding studies of cobalt(III) mixed-polypyridyl complex. *J Inorg Biochem* 1997;68:79–83.
25. Zhang QL, Liu JG, Chao H, Xue GQ, Ji LN. DNA-binding and photocleavage studies of cobalt(III) polypyridyl complexes: $[\text{Co}(\text{phen})_2\text{IP}]^{3+}$ and $[\text{Co}(\text{phen})_2\text{PIP}]^{3+}$. *J Inorg Biochem* 2001;83:49–55.
26. Shi S, Liu J, Li J, Zheng K, Huang X, Tan C, Chen L, Ji L. Synthesis, characterization and DNA-binding of novel chiral complexes Δ - and Λ - $[\text{Ru}(\text{bpy})_2\text{L}]^{2+}$ (L = o-mopip and p-mopip). *J Inorg Biochem* 2006;100:385–395.
27. Wolfe A, Shimer GH Jr., Meehan T. Polycyclic aromatic hydrocarbons physically intercalate into duplex regions of denatured DNA. *Biochem* 1987;26:6392–6396.
28. Ihmels H, Otto D. Intercalation of organic dye molecules into double-stranded DNA –General principles and recent developments. *Top Curr Chem* 2005;258:161–204.
29. Basili S, Bergen A, Dall'Acqua F, Faccio A, Ranzhan A, Ihmels H, Moro S, Viola G. Relationship between the structure and the DNA binding properties of diazoniapolycyclic duplex- and triplex-DNA binders: Efficiency, selectivity, and binding mode. *Biochem* 2007;46:12721–12736.
30. Huguet AI, Manez S, Alcaraz MJ. Superoxide scavenging properties of flavonoids in a non-enzymic system. *Z Naturforsch* 1990;45:19–24.
31. Le X, Liao S, Liu X, Feng X. Synthesis, structure and SOD-like activity of a ternary Cu(II) complex with 1,10-phenanthroline and L-valinate. *J Coord Chem* 2006;59:985–995.
32. Mendham J, Denney RC, Barnes JD, Thomas MJK. *Vogel's Text Book of Quantitative Chemical Analysis*, 6th ed. Singapore: Pearson Education PVT, 2002:312–460.
33. Day RA Jr, Underwood AL. *Quantitative Analysis*, 6th ed. Prentice-Hall of India PVT, 2006:388–441.
34. Furniss BS, Hannaford AJ, Smith PWG, Tatchell AR, *Vogel's Textbook of Practical Organic Chemistry*, 5th ed. Harlow: Longman, 2004.
35. Chohan ZH, Supuran CT, Scozzafava A. Metal binding and antibacterial activity of ciprofloxacin complexes. *J Enzyme Inhib Med Chem* 2005;20:303–307.
36. Deacon GB, Philips RJ. Relationships between the carbon-oxygen stretching frequencies of carboxylato complexes and the type of carboxylate coordination. *Coord Chem Rev* 1980;33:227–250.
37. Nakamoto K. *Infrared and Raman Spectra of Inorganic and Coordination Compounds*, 4th ed. New York: A Wiley Interscience Publication, 1986.
38. Patel SH, Pansuriya PB, Chhasatia MR, Parekh HM, Patel MN. Coordination chain polymeric assemblies of trivalent lanthanides with multidentate schiff base synthetic, spectral investigation and thermal aspects. *J Therm Anal Cal* 2008;91:413–414.
39. Turel I, Leban I, Bukovec N. Crystal structure and characterization of the bismuth (III) compound with quinolone family member (ciprofloxacin). Antibacterial study. *J Inorg Biochem* 1997;66:241–245.
40. Freedman HH. Intramolecular H-bonds. I. A spectroscopic study of the hydrogen bond between hydroxyl and nitrogen. *J Am Chem Soc* 1961;83:2900–2905.
41. Iskander MF, El-Sayed L, Salem NMH, Warner RW. Synthesis, characterization and magnetochemical studies of dicopper(II) complexes derived from bis(N-salicylidene)dicarboxylic acid dihydrazides. *J Coord Chem* 2005;58:125–139.
42. Mendoza-Diaz G, Martineza-Aguilera LMR, Perez-Alonso R, Solans X, Moreno-Esparza R. Synthesis and characterization of mixed ligand complexes of copper with nalidixic acid and (N-N) donors. Crystal structure of $[\text{Cu}(\text{Phen})(\text{Nal})-(\text{H}_2\text{O})]\text{NO}_3 \cdot 3\text{H}_2\text{O}$. *Inorg Chim Acta* 1987;138:41–47.
43. Wang LY, Chen QY, Huang J, Wang K, Feng CJ, Gen ZR. Synthesis, characterization, and bioactivities of copper complexes with N-substituted di(picolyl) amine. *Trans Met Chem* 2009;34:337–345.
44. Mautner FA, Vicente R, Louka FRY, Massoud SS. Dinuclear fumarato- and terephthalato- bridged copper(II) complexes; structural characterization and magnetic properties. *Inorg Chim Acta* 2008;361:1339–1348.
45. Carballo R, Castineiras A, Covelo B, Garcia-Martinez E, Niclos J, Vazquez-Lopez EM. Solid state coordination chemistry of mononuclear mixed-ligand complexes of Ni(II), Cu(II) and Zn(II) with α -hydroxycarboxylic acids and imidazole. *Polyhedron* 2004;23:1505–1518.
46. Figgis BN, Lewis J, In Lewis J, Wilkins RG, eds. *Modern Coordination Chemistry: Principles and Methods*. New York: Interscience, 1960.
47. Psomas G, Dendrinou-Samara C, Philippakopoulos P, Tangoulis V, Raptoulou CP, Samaras EI, Kessissoglou DP. CuII-herbicide complexes: Structure and bioactivity. *Inorg chim Acta* 1998;272:24–32.
48. Silverstein RM, Webster FX. *Spectrometric Identification of Organic Compounds*. 6th ed. New York: John Wiley and Sons:2004.
49. Dendrinou-Samara C, Psomas G, Raptoulou CP, Kessissoglou DP. Copper(II) complexes with phenoxyalkanoic acids and nitrogen donor heterocyclic ligands: structure and bioactivity. *J Inorg Biochem* 2001;83:7–16.
50. Russell AD. Principles of antimicrobial activity. In: Block SS, ed. *Disinfection, Sterilization and Preservation*. 4th ed. Philadelphia: Lea and Febinger, 1991:27–59.
51. Rossmore HW. Biocides for metal working lubricants and hydraulic fluids. In: Block SS, ed. *Disinfection, Sterilization and Preservation*. 4th ed. Philadelphia: Lea and Febinger, 1991:290–321.
52. Rodger A, Norden B. ed. *Circular Dichroism and Linear Dichroism*, Oxford: Oxford University Press;1997.
53. Song G, He Y, Cai Z. The interaction between levofloxacin hydrochloride and DNA mediated by Cu^{2+} . *J Fluoresc* 2004;14:705–710.
54. Jenkins TC. in: Fox KR, ed. *Drug-DNA Interaction Protocols*. Totowa, New Jersey: Humana Press, 1997:195–218.
55. Son GS, Yeo JA, Kim MS, Kim SK, Holmen A, Akerman B, Norden B. Binding mode of norfloxacin to calf thymus DNA. *J Am Chem Soc* 1998;120:6451–6457.
56. El-Metwaly NM. Spectral and biological investigation of 5-hydroxyl-3-oxopyrazoline 1-carbothiohydrazide and its transition metal complexes. *Trans Met Chem* 2007;32:88–94.
57. Palchaudhuri R, Hergenrother PJ. DNA as a target for anticancer compounds: methods to determine the mode of binding and the mechanism of action. *Curr Opin Biotech* 2007;18:497–503.
58. Wheate NJ, Brodie CR, Collins JG, Kemp S, Aldrich-Wright JR. DNA intercalators in cancer therapy: organic drugs and their spectroscopic tools of analysis. *Mini-Rev Med Chem* 2007;7:627–684.
59. Hertzberg RP, Dervan PB. Cleavage of double helical DNA by methidium-propyl-EDTA-iron(II). *J Am Chem Soc* 1982;104:313–315.
60. Sigman DS, Graham DR, Marshall LE, Reich KA. Cleavage of DNA by coordination complexes. Superoxide formation in the oxidation of 1,10-phenanthroline-cuprous complexes by oxygen-relevance to DNA-cleavage reaction. *J Am Chem Soc* 1980;102:5419–5421.
61. Figgis BN, Nyholm RS. A convenient solid for calibration of the Gouy susceptibility apparatus. *J Chem Soc* 1958;4190–4191.